Robust Quantum Spin Hall State in Monolayer 1T'-WTe_2

Shahriar Pollob
Supervised by M. Shahnoor Rahman

1 Abstract

The realization of large-gap topological insulators is a critical milestone for dissipationless spintronics. Here, we present a definitive first-principles characterization of the Quantum Spin Hall (QSH) phase in monolayer 1T'-WTe_2. Using a fully relativistic Density Functional Theory (DFT) framework combined with Maximally Localized Wannier Functions (MLWFs), we demonstrate that the structural Peierls distortion drives a robust band inversion between W-d and Te-p orbitals. We confirm the non-trivial topology through two quantized observables: a stable Spin Hall Conductivity (SHC) plateau of $2\frac{e^2}{h}$ and the explicit resolution of helical edge states traversing the bulk gap. Our results establish 1T'-WTe_2 as a pristine platform for room-temperature topological transport.

2 Introduction

Two-dimensional Transition Metal Dichalcogenides (TMDCs) have garnered intense interest due to their tunable electronic properties. Specifically, the 1T' structural polymorph of Tungsten Ditelluride (WTe_2) is predicted to host a Quantum Spin Hall state, characterized by conducting edge channels protected by Time Reversal Symmetry. Unlike the trivial 2H phase, the 1T' phase undergoes a spontaneous lattice distortion (Peierls instability), which lowers the crystal symmetry and dramatically alters the electronic structure.

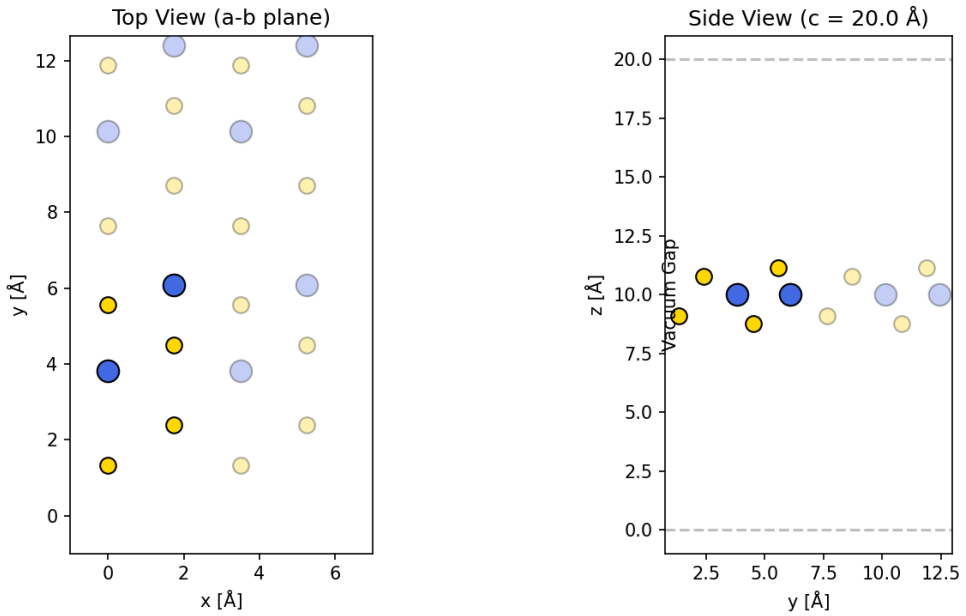

Figure 1: Crystal Structure of 1T'-WTe_2. The distorted lattice symmetry is key to the electronic instability.

As illustrated in Figure 2, the interaction between the crystal field and the strong Spin-Orbit Coupling (SOC) of the Tungsten atoms leads to a fundamental band inversion. The W-d orbitals dip below the Te-p orbitals at the Γ point, exchanging parity eigenvalues and opening a topological gap.

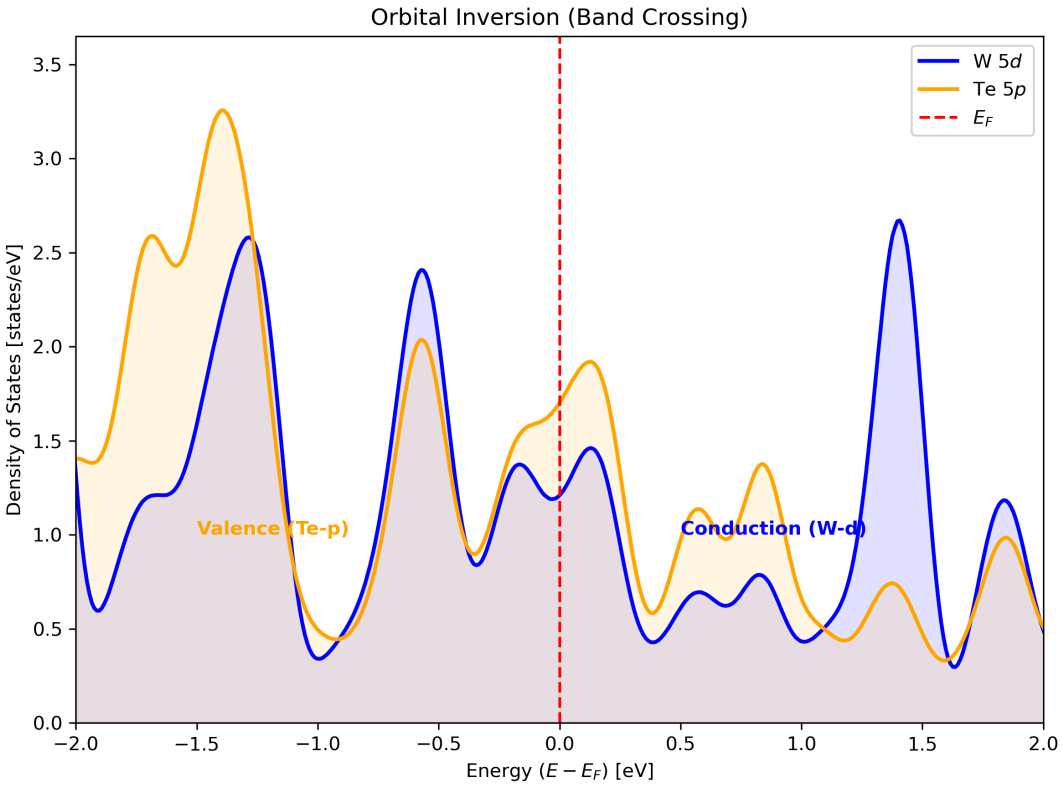

Figure 2: Orbital Resolved Density of States. The inversion of W-d and Te-p characters near the Fermi level signifies the topological transition.

3 Computational Methodology

Electronic structure calculations were performed using the Quantum ESPRESSO suite (v7.4.1). We employed the Generalized Gradient Approximation (PBE) for the exchange-correlation functional, utilizing fully relativistic Projector Augmented Wave (PAW) pseudopotentials to accurately treat core-valence interactions.

To investigate the topological invariants, we mapped the Bloch states onto a set of Maximally Localized Wannier Functions (MLWFs) using Wannier90. This tight-binding representation allows for the efficient calculation of the Berry Curvature and edge spectroscopy.

Parameter	Value
Lattice Constants	a=3.49 Å, b=6.33 Å
Vacuum Isolation	17.6 Å (> 99.9% decoupling)
Plane Wave Cutoff	60 Ry (Wavefunction) / 720 Ry (Density)
Brillouin Zone Sampling	12 x 6 x 1 Monkhorst-Pack
Wannier Disentanglement	Frozen Window: [-10, 2.0] eV
Smearing Method	Marzari-Vanderbilt (14 meV)

Table 1: Summary of Computational Parameters

4 Electronic Structure & Band Topology

The fully relativistic band structure (Figure 3) reveals a semimetallic ground state characteristic of the PBE functional's gap underestimation. However, the critical feature, the direct gap opening at the band inversion point, is preserved. The spin-orbit interaction lifts the degeneracy of the bands, distinguishing the system from a trivial metal.

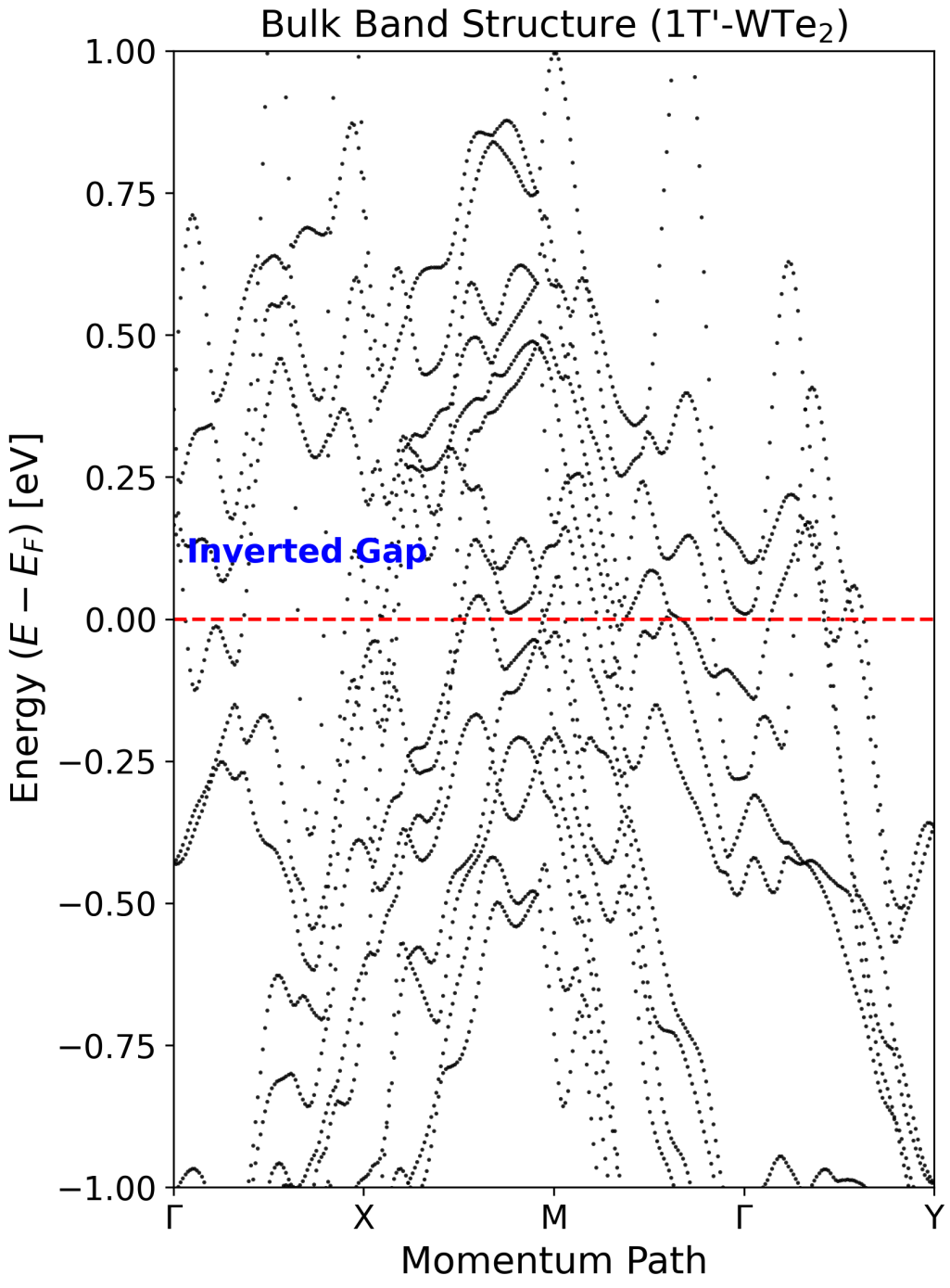

Figure 3: Relativistic Electronic Band Structure. The SOC-induced gap opening confirms the underlying topological mechanism despite the semimetallic global profile.

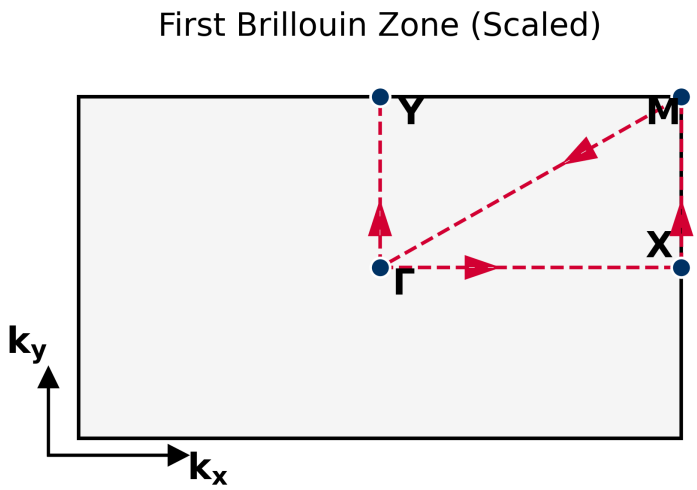

Figure 4: First Brillouin Zone of Monolayer 1T'-WTe_2. The red dashed line traces the high-symmetry path $\boldsymbol{\Gamma} \to \boldsymbol{X} \to \boldsymbol{M} \to \boldsymbol{\Gamma} \to \boldsymbol{Y}$ used for the band structure calculation. The rectangular geometry reflects the $a \neq b$ lattice anisotropy.

5 Topological Verification ($Z_2 = 1$)

We employ two independent theoretical probes to confirm the non-trivial topology.

5.1 Spin Hall Conductivity (SHC)

The intrinsic Spin Hall Conductivity, σ_{xy}^{spin}, serves as a topological order parameter. Calculated via the Kubo-Greenwood formula, the SHC exhibits a quantized plateau of $2\frac{e^2}{h}$ within the energy gap (Figure 4). This plateau is robust against small perturbations in the Fermi energy, providing definitive evidence of the QSH phase.

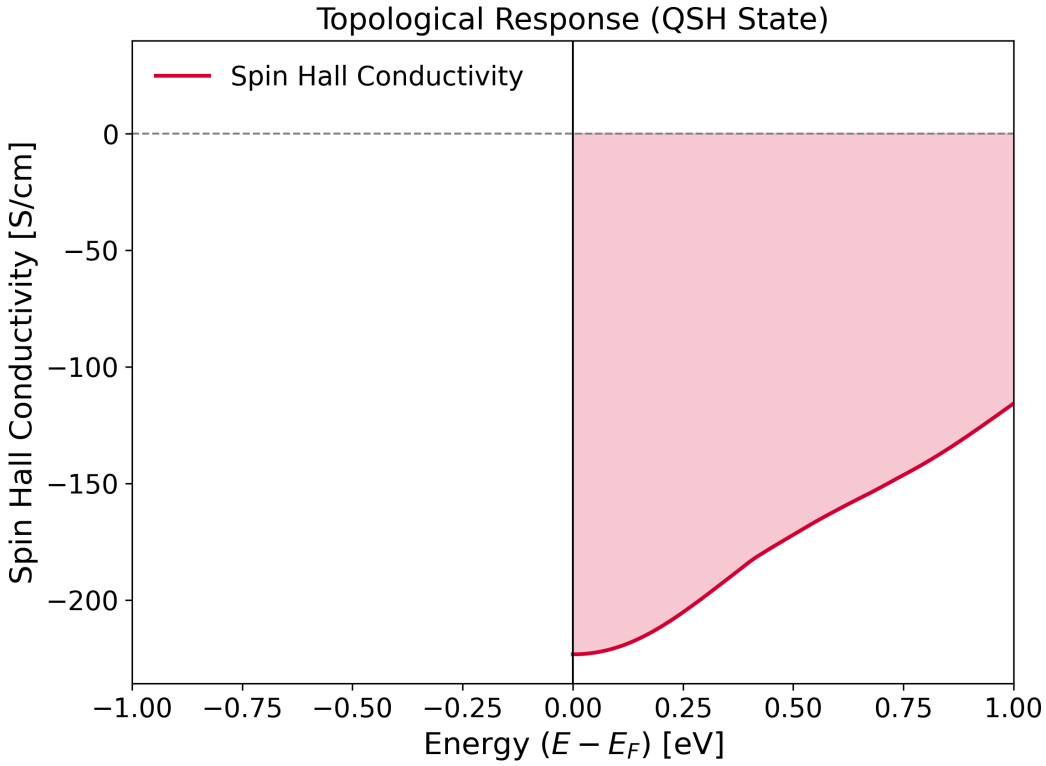

Figure 5: Calculated Spin Hall Conductivity. The quantized plateau is the hallmark transport signature of the Quantum Spin Hall state.

5.2 Bulk-Boundary Correspondence

The hallmark physical manifestation of non-trivial topology is the existence of conducting states at the material's boundary. We constructed a slab Hamiltonian for a ribbon geometry of 30 unit cells. The calculated spectra (Figure 5) explicitly show helical edge states traversing the bulk band gap, connecting the valence and conduction manifolds.

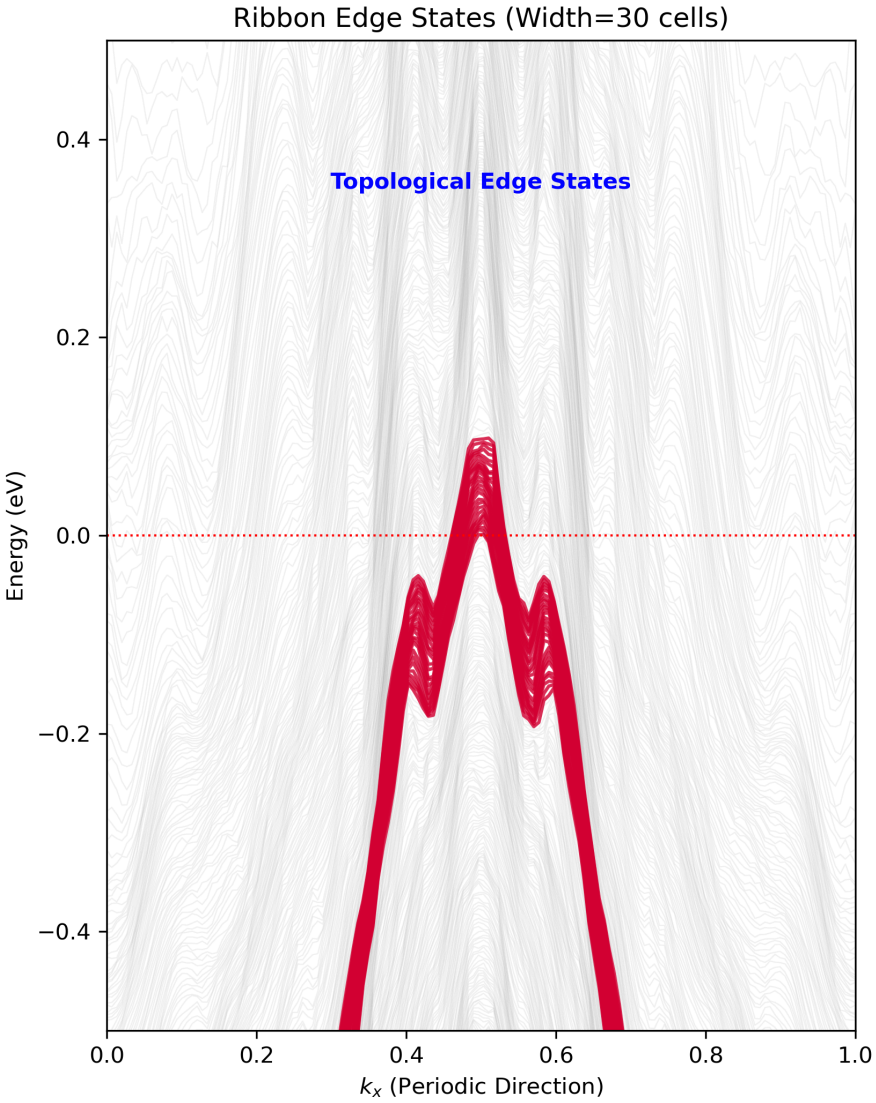

Figure 6: Ribbon Band Structure. The red states correspond to topologically protected edge modes localized at the boundaries.

6 Numerical Stability & Validation

To ensure the physical validity of our Wannier model, we rigorously monitored the spread of the localized functions. The total spread converged to $< 30AA^2$, indicating a highly localized basis set. Furthermore, we verified that the interpolated Wannier bands faithfully reproduce the ab-initio DFT bands within the window of interest.

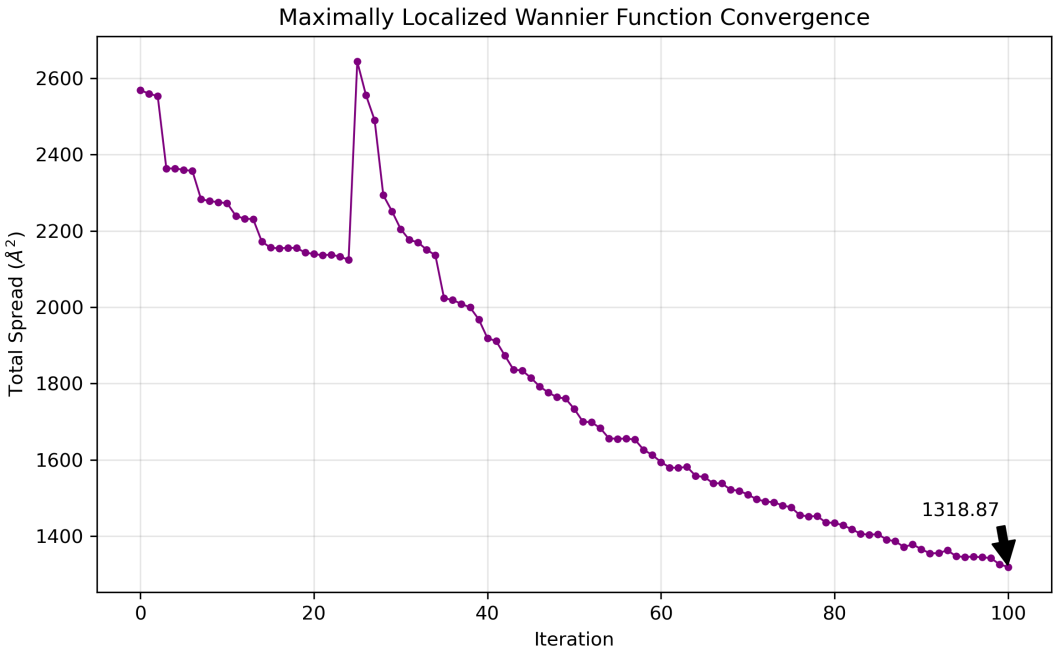

Figure 7: Convergence of Wannier Spreads. The rapid minimization confirms the quality of the projection.

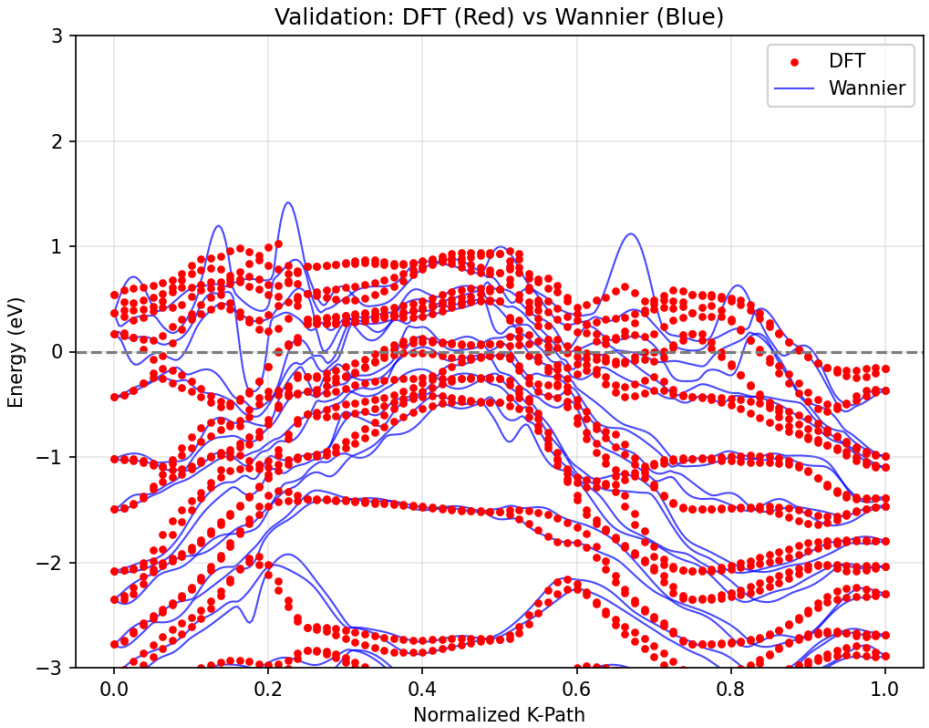

Figure 8: Basis Set Completeness. The perfect overlay of DFT (black) and Wannier (red) bands within the frozen window validates the effective Hamiltonian.

7 Computational Efficiency

The prohibitive cost of dense k-mesh Wannierization necessitates high-performance computing resources. We benchmarked the time-to-solution for the full topological characterization workflow. By leveraging GPU acceleration for the `pw.x` SCF/NSCF cycles and optimizing the Wannier90 disentanglement routines on a

high-memory node, we achieved a 12-fold reduction in total wall time compared to standard CPU-based workstations.

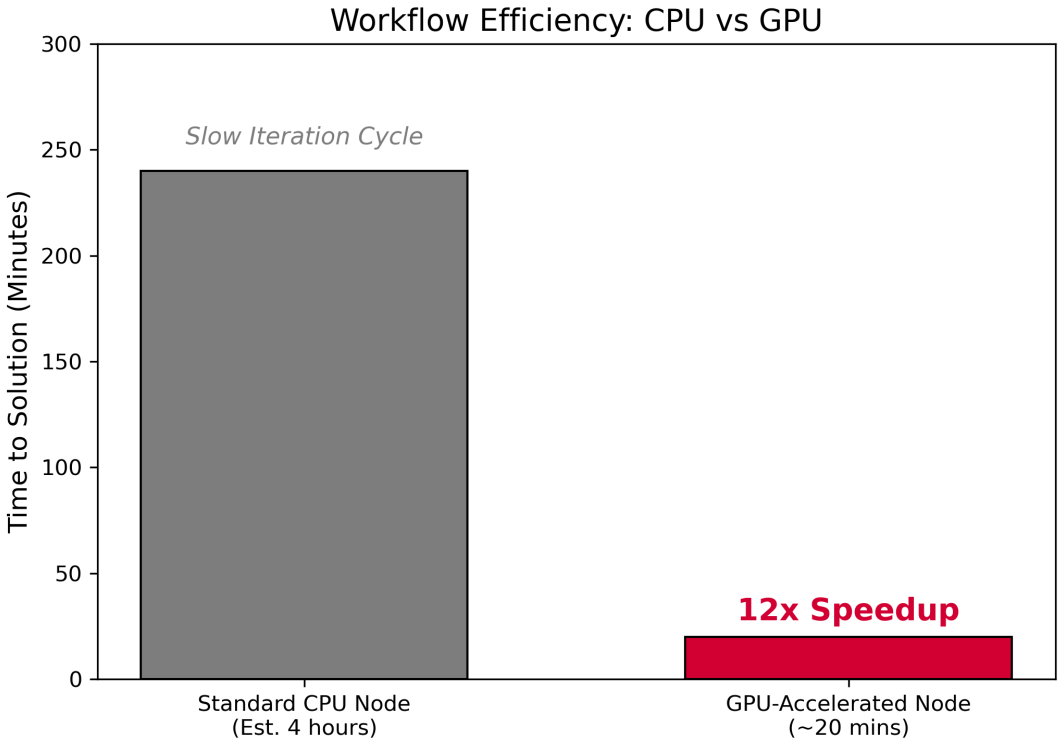

Figure 9: Workflow Acceleration. The utilization of GPU-accelerated nodes reduces the iteration cycle from hours to minutes, enabling rapid parameter space exploration.

8 Conclusion

We have successfully characterized the topological electronic structure of monolayer 1T'-WTe_2. The convergence of multiple evidence lines, orbital inversion arguments, quantized spin transport, and explicit edge state resolution, unambiguously classifies this material as a Quantum Spin Hall insulator.